Ultrasonics Sonochemistry 91 (2022) 106225

Contents lists available at ScienceDirect

Ultrasonics Sonochemistry

journal homepage: www.elsevier.com/locate/ultson

Thermoultrasound and microwave-assisted freeze-thaw pretreatments for improving infrared drying and quality characteristics of red dragon fruit slices

Edidiong Joseph Bassey [a,b,c], Jun-Hu Cheng [a,b,c], Da-Wen Sun [a,b,c,d,*]

[a] School of Food Science and Engineering, South China University of Technology, Guangzhou 510641, China
[b] Academy of Contemporary Food Engineering, South China University of Technology, Guangzhou Higher Education Mega Center, Guangzhou 510006, China
[c] Engineering and Technological Research Centre of Guangdong Province on Intelligent Sensing and Process Control of Cold Chain Foods, and Guangdong Province Engineering Laboratory for Intelligent Cold Chain Logistics Equipment for Agricultural Products, Guangzhou Higher Education Mega Centre, Guangzhou 510006, China
[d] Food Refrigeration and Computerized Food Technology, University College Dublin, National University of Ireland, Agriculture and Food Science Centre, Belfield, Dublin 4, Ireland

ARTICLE INFO

Keywords:
Ultrasound
Microwave
Freeze-thaw
Infrared drying
Antioxidant activity
Bioactive compounds

ABSTRACT

The effects of thermoultrasound (US-FT), microwave (MW-FT), and room temperature (RT-FT) freeze–thaw pretreatments were evaluated for improving drying kinetics and quality during infrared drying (IRD) of red dragon fruit slices (RDFS). Results indicated that microstructural alterations induced by the different pretreatments improved the moisture removal rate and effective diffusivity, and significantly reduced the drying time. US-FT pretreatments prompted more efficient drying and presented an overall enhancement in the quality of RDFS, particularly at low temperatures of 25 and 50 °C, while enhancements in TFC, FRAP, and CUPRAC were associated with RT-FT. High-power (500 W) MW-FT pretreatments improved colour and structural properties, while low-power (100, 300 W) improved TPC, TFC, ascorbic acid, betalains, and antioxidant activity. Overall, cellular and chemical alterations prompted by pretreatments improved the drying process but presented adverse effects on betaxanthin. The study presented the fundamental background for improving the IRD of foods from the use of improved thawing approaches during freeze–thaw pretreatments.

1. Introduction

Drying is the oldest, most effective, and most broadly utilized technique for reducing water content and improving postharvest utilization of biological materials. Aside from shelf life extension, drying also enhances the nutritional and economic value of food products [28]. However, extended drying durations can lead to low energy efficiency and undesirable physical and chemical changes in food products. Therefore, innovative drying approaches that can shorten the drying time and improve the overall drying efficiency and quality of biological materials are necessary [10]. Accordingly, alternative drying approaches like infrared drying (IRD) are continuously being evaluated for improving the drying of biological materials [2].

IRD involves the transfer, absorption, and conversion of radiative energy to sensible heat by the vibration of polar molecules within the heated material that results in volumetric heating and accelerated heat and mass transfer rate, and presents advantages of high energy efficiency and improved product quality over conventional drying systems [2,5]. Even so, uneven radiation absorption and limited penetration depth of radiative energy which results in inhomogeneous and localized overheating and quality deterioration might be associated with IRD of biological materials [11]. Previous studies have projected that the application of pretreatments can mitigate these drawbacks, and in particular, freeze–thaw (FT) pretreatments have been demonstrated to induce structural alterations in food materials for reducing drying time and enhancing physicochemical and bioactive properties of the final products [11,5,36]. The structural modifications were reported to be induced by the creation of intracellular pores caused by ice crystals formation during freezing and subsequent thawing, leading to overall improvements in the drying process [10,34].

Despite the promising results reported by these studies, some quality degradation linked with excessive structural deformations and resultant

* Corresponding author at: School of Food Science and Engineering, South China University of Technology, Guangzhou 510641, China.
E-mail address: dawen.sun@ucd.ie (D.-W. Sun).
URL: http://www.ucd.ie/refrig;%20http://www.ucd.ie/sun (D.-W. Sun).

https://doi.org/10.1016/j.ultsonch.2022.106225
Received 3 August 2022; Received in revised form 11 October 2022; Accepted 6 November 2022
Available online 7 November 2022

leaching loss has been associated with the use of FT pretreatments [6]. For example, FT pretreatment was reported to cause damage to the cell wall, leading to increased shrinkage, enzymatic browning, undesirable changes in colour, and losses in phytochemicals during infrared-hot air drying of lotus and microwave drying of *Platycodon grandiflorum* [16,36]. Nevertheless, improved thawing approaches targeting reducing the thawing time for preserving cell structures and components can reduce the negative effects of FT pretreatments on food quality during drying [6]. Therefore, selecting appropriate thawing methods and conditions during FT pretreatment is essential for improving the drying characteristics and quality of dried products.

Emerging thawing methods such as ultrasound (US) and microwave (MW) thawing have been explored for mitigating undesirable physicochemical and chemical changes in the functional properties of biological materials during FT treatments [6]. Ultrasound thawing has been reported to provide uniform and rapid thawing of food from enhanced heat transfer due to the rapid reduction of ultrasonic waves close to the frozen/thawed boundary, asymmetric collapse of the bubble, sponge effects and the conversion of sound energy to heat energy, while microwave thawing has been employed commercially and domestically due to high efficiency, fast thawing rate, ease of use, and minimal structural collapse, while [7,29]. However, sample discolouration and loss of bioactive compounds caused by the formation of free radicals and critical cell rupture might be associated with ultrasound thawing, while localized heating and limited thermal conversion might be associated with microwave thawing [8,7]. These drawbacks can be addressed by selecting appropriate ultrasound and microwave thawing conditions of power, exposure time, and temperatures to achieve a twofold advantage of improved energy efficiency and improved quality of the final product.

Therefore, this study was designed to investigate the effects of thermoultrasound and microwave-assisted freeze–thaw pretreatments on the drying characteristics and quality of red dragon fruit slices (RDFS) during infrared drying. To the best of our knowledge, this is the first study to evaluate the suitability of thermoultrasound and microwave-assisted thawing for improving freeze–thaw pretreatments and ameliorating drying kinetics and quality during IRD of biological materials.

2. Materials and methods

2.1. Chemicals and reagents

Methanol (CH_3OH) and ethanol (C_2H_5OH) were bought from Tianjin Fuyu Fine Chemical Co., ltd. (Tianjin, China). Folin-Ciocialteu reagent (FCR) was acquired from Sangon Biotech Co., ltd. (Shanghai, China). Sodium carbonate (Na_2CO_3) and ammonium acetate ($C_2H_7NO_2$) were purchased from Guangzhou Chemical Reagent Factory (Guangzhou, China), and hydrogen peroxide (H_2O_2) was procured from Chron Chemicals (Chengdu, China). 6-hydroxy-2,5,7,8-tetramethylchroman-2-carboxylic acid (Trolox, $C_{14}H_{18}O_4$), metaphosphoric acid (HPO_3), neocuproine ($C_{14}H_{12}N_2$), aluminium chloride ($AlCl_3$), sodium acetate ($C_2H_3NaO_2$), potassium persulfate ($K_2S_2O_8$), salicylic acid ($C_7H_6O_3$), 2,4,6-Tris(2-pyridyl)-s-triazine (TPTZ: $C_{18}H_{12}N_6$), and quercetin ($C_{15}H_{10}O_7$) were supplied by Aladdin Biochemical Technology Co., ltd. (Shanghai, China). Sodium nitrite ($NaNO_2$) was purchased from Lingfeng Chemical Reagent Co., ltd. (Shanghai, China). 2,2′-Azino-bis (3-ethylbenzothiazoline-6-sulfonic acid) (ABTS: $C_{18}H_{18}N_4O_6S_4$), Ascorbic acid ($C_6H_8O_6$), 2,6-dichlorophenolindophenol ($C_{12}H_7NCl_2O_2$), ferrous sulfate ($FeSO_4$), copper dichloride ($CuCl_2$), sodium hydroxide (NaOH), ferric chloride ($FeCl_3$), sodium chloride (NaCl), and gallic acid ($C_7H_6O_5$) were procured from Shanghai Macklin Biochemical Co., ltd. (Shanghai, China).

2.2. Sample preparation and pretreatments

Red dragon fruits were purchased from a local market (Guangzhou, China), which were washed and stored in a refrigerator (BCD-525WKPZM(E), Hefei Midea Refrigeration Co., ltd., Hefei, China) at 4 °C pending experiments. Fruits were peeled and cut into thin slices (RDFS) of 70 mm diameter and 5 mm thick and frozen in a conventional freezer (BCD-525WKPZM(E), Hefei Midea Refrigeration Co., ltd., Hefei, China) at −20 °C for 12 h. Thermoultrasound-assisted freeze–thaw (US-FT) treatment was achieved by thawing the frozen samples in a bath-type sonochemical reactor (SB25-12D, Ningbo Xinzhi Ultrasonic Equipment Co., ltd., Ningbo, China) operating at acoustic power of 500 W, frequency of 40 kHz and, temperature levels of 25, 50, and 70 °C, and the treated samples were collectively designated as US-FTS or US25S, US50S, and US70S, respectively. For the microwave-assisted freeze–thaw (MW-FT) treatment, a domestic microwave oven (PG2311W, Guangdong Midea Kitchen Appliance Manufacturing Co., ltd, Foshan, Guangdong, China.) with a frequency of 2450 MHz and total power of 1000 W was employed for thawing the frozen samples at power levels of 100, 300, and 500 W, and the treated samples were collectively designated as MW-FTS, or MW1S, MW3S, and MW5S, respectively. Some frozen samples were also thawed at room temperature of 25 °C (RT-FT) and the samples were designated as RTS. The thawing process was completed when the temperature at the centre of the samples reached 25 ± 2 °C, and the thawing times of the samples were 7, 4, and 2 min for MW1S, MW3S, and MW5S, and 30, 8, and 4 min for US25S, US50S, and US70S, respectively, and 180 min for RTS. The RDFS without freeze–thaw treatments served as control and were designated as CTRS. The drip loss of the pretreated samples was determined before drying according to the method outlined by Peng et al. [22].

2.3. Drying experiment

A laboratory-scale infrared dryer (GP1500-3, Gaopeng Automation Equipment Co., ltd., Suzhou, China) equipped with 900 W infrared emitters, a digital control unit, and a rotatable tray was employed for the drying experiments. Approximately 50 g of frozen-thawed RDFS were spread in a thin layer on the drying tray and dried at a fixed temperature, tray rotation speed, and irradiation distance of 60 °C, 40 rpm, and 20 cm, respectively. The changes in the weight of the samples during drying were recorded at 20 min intervals at the beginning of drying and at a 30 min interval as drying progressed, and the drying process was completed when there were no significant changes in sample weight over two consecutive time intervals.

2.4. Drying kinetics

Moisture ratio (MR) was evaluated based on the initial moisture, equilibrium moisture, and moisture content of samples at drying intervals and computed according to the following equation [37]:

$$MR = \frac{M_t - M_e}{M_o - M_e} \quad (1)$$

where MR, M_o, $M_e$and $M_t a$re the moisture ratio, initial moisture content, equilibrium moisture content (g water/g dry mass), and moisture content at drying time t (min), respectively.

The effective moisture diffusivity was evaluated based on Fick's second law of diffusion and was calculated using the following equation:

$$MR = \frac{8}{\pi^2}\sum_{n=0}^{\infty}\frac{1}{(2n+1)^2}\exp\left(-(2n+1)^2\frac{\pi^2 D_{eff}{}^t}{4L^2}\right) \quad (2)$$

where n is the number of terms of the Fourier series, D_{eff} is the effective moisture diffusivity (m^2/s), and L is the half slab thickness of the sample slices (m).

Equation (2) can be further simplified to a finite diffusion equation for extended drying duration, as shown below:

$$ln(MR) = \frac{8}{\pi^2} exp\left\{\frac{-\pi^2 D_{eff}{}^t}{4L^2}\right\} \quad (3)$$

The slope obtained from the plot of *ln MR* versus time from Eq. (3) was used for calculating the D_{eff} as shown below:

$$K = \frac{\pi^2 D_{eff}}{4L^2} \quad (4)$$

2.5. Physicochemical quality analysis

2.5.1. Rehydration ratio (RR)

The RR was evaluated by placing 1 g of dried sample in a 100 mL flask containing 50 mL distilled water for 1 h at room temperature of 25 °C. Subsequently, the excess water was blotted from the surface of the samples using absorbent paper before weighing, and the rehydration ratio was calculated as the ratio of the mass of rehydrated samples to dried samples [5].

2.5.2. Determination of degree of shrinkage

Sample shrinkage was determined in relation to the changes in the diameter, thickness, and area of samples after drying using the following equations [25]:

$$Diametershrinkage(DS) = \frac{D_0 - D}{D_0} \times 100 \quad (6)$$

$$Thicknessshrinkage(TS) = \frac{T_o - T}{T_o} \times 100 \quad (7)$$

$$Areashrinkage(AS) = \frac{A_o - A}{A_0} \times 100 \quad (8)$$

where D_0, T_0, and A_0 represent the initial diameter (cm), thickness (cm), and area (cm^2) of the samples, respectively, and *D, T*, and *A* represent the diameter, thickness, and area of samples after drying.

2.5.3. Texture analysis

The texture of the samples was determined in terms of the hardness values from a penetration test using a texture analyzer (TA. XT Plus, Stable Micro Systems ltd., Surrey, UK) equipped with a 2 mm diameter cylindrical probe and a 50 kg load cell. The test, pre-test and post-test speeds were set to 1, 3 and 3 mm/s, respectively at a triggering force of 490.3 N [39].

2.6. Analysis of phytochemical composition and antioxidant activities

2.6.1. Extraction procedure

For the determination of total phenolic content (TPC), total flavonoid content (TFC), and antioxidant activity (AA). 0.5 g of powdered samples were extracted thrice in 10 mL of 80 % CH_3OH for 1 h in a shaking water bath (DKZ-2B, Shanghai Yiheng Scientific Instrument Co., ltd., Shanghai, China) at a temperature of 30 °C [5]. The resultant solution was centrifuged (JW-3024HR, Anhui Jiaven Equipment Industry Co., ltd., Hefei, China) for 30 min at 10,000 rpm and 4 °C, and the supernatants were filtered and stored at 4 °C until further analysis.

2.6.2. Total phenolic and flavonoid contents

The TPC was determined according to the Folin-Ciocalteu method described in our previous study [5]. Briefly, 0.2 mL of sample was combined with 3 mL of 10 % Folin-Ciocalteu reagent, and 1.5 mL of 20 % Na_2CO_3 was added after 8 min. Thereafter, the mixture was incubated for 90 min at a room temperature of 25 °C, and the absorbance was read at 765 nm using a UV spectrophotometer (UV-1800, Shimadzu Co., Kyoto, Japan). Results were expressed as milligrams of gallic acid equivalents per gram samples (mg GAE/00 g) from a gallic acid calibration curve (y = 0.0033x + 0.0135).

The TFC was evaluated using the colourimetric method outlined in our previous study [5]. Briefly, 1 mL of the extract was combined with 0.3 mL of 5 % $NaNO_2$ and allowed to stand for 5 min. Afterwards, 0.3 mL of 10 % $AlCl_3$ was added and incubated for 5 min before adding 2 mL of 1 M NaOH. The absorbance of the mixture was measured at 510 nm after incubation for 10 min, and the results were expressed as quercetin equivalent per gram of the samples (QUE/g) from a quercetin calibration curve (y = 0.0008x + 0.0376).

2.6.3. Ascorbic acid content

The ascorbic acid content (AAC) was measured according to the method described in a previous study [31]. Briefly, 1 g of pulverized sample was extracted with 10 mL of 3 % HPO_3, centrifuged for 30 min at 10000 rpm and 4 °C, and filtered. Thereafter, 1 mL of the filtrate was combined with 9 mL of 0.0025 % $C_{12}H_7NCl_2O_2$ and incubated for 30 min at 25 °C. The absorbance was measured at 518 nm, and the AAC was calculated using the AAC calibration curve (y = -0.0274x + 3.2081) and expressed in milligrams per gram of samples (mg/g).

2.6.4. Betalain quantification

The betalain content was determined according to the procedure described in our previous study [5]. Briefly, 1 g of sample was extracted thrice with 10 mL of 50 % C_2H_5OH in a shaking water bath at 25 °C for 1 h and centrifuged at 10000 rpm and 25 °C for 10 min. The absorbance of the filtrate was read at 538 and 480 nm to determine the betacyanin, and betaxanthin contents, respectively, and the specific betalains were calculated and expressed as mg/g using the following equation:

$$Betalaincontent(\%) = \frac{A \times DF \times MW \times V}{\varepsilon \times L \times W} \times 100 \quad (9)$$

where *A* is the absorbance of extract, *DF* is the dilution factor of extract solution, *MW* is the molecular weight of betaxanthin (308 g mol^{-}) or betacyanin (550 g mol^{-1}), *V* is the volume of extract, ε is the molar extinction coefficient of betacyanin (60 000 l mol^{-1} cm^{-1}) or betaxanthin (48 000 l mol^{-1} cm^{-1}), *W* is the weight of extracted samples, and *L* is the path length of the cuvette (1 cm).

2.6.5. Antioxidant activity

The ABTS radicals scavenging, hydroxyl radicals scavenging activity (HRSA), cupric ion reducing antioxidant capacity (CUPRAC) and ferric reducing antioxidant power (FRAP) methods were used to evaluate the antioxidant capacity of RDFS. The ABTS was assayed from the method reported by Zhang et al. [36] with slight modifications. A stock solution was prepared by mixing 166 µL of 140 mmol $K_2S_2O_8$ with 10 mL of 7 mM $C_{18}H_{18}N_4O_6S_4$ and stored overnight at 25 °C. The working solution was prepared by diluting 0.95 mL stock solution with distilled water to an absorbance value of 0.700 ± 0.005 at 734 nm. Thereafter, 360 µL of the working solution was combined with 40 µL of extracts and allowed to react for 10 min at 25 °C, and the absorbance was measured at 734 nm. The ABTS antioxidant capacity of the samples was expressed as micromole Trolox equivalent (µmol TE/g) from a Trolox calibration curve (y = -0.0164x + 0.595).

The HRSA was assayed using the procedure of Wu et al. (2019) with minor modifications. Briefly, 1 mL of sample extract was combined with 1 mL of 9 mM $FeSO_4$ and 1 mL of 9 mM $C_7H_6O_3$ solution. Subsequently, 1 mL of 8.8 mM H_2O_2 was added, mixed vigorously, and incubated for 30 min at 37 °C before absorbance reading at 510 nm. The HRSA was calculated from the following equation:

$$HRSA(\%) = \frac{Abs_{control} - (Abs_{Sample} - Abs_{blank})}{Abs_{control}} \times 100 \quad (10)$$

where $Abs_{control}$ is the absorbance of reagents and distilled water; Abs_{Sample} is the absorbance of reagents and sample extract solution; Abs_{blank} is the absorbance of reagents without hydrogen peroxide.

The CUPRAC was assayed from the method outlined by Kayacan et al. [13]. Briefly, 150 µL of extract diluent was mixed with 1 mL of

10 mM $CuCl_2$, 1 mL of 1 M $C_2H_7NO_2$, 1 mL of 7.5 mM $C_{14}H_{12}N_2$, and 1 mL of distilled water. Thereafter, the mixture was incubated for 1 h before absorbance reading at 450 nm. The results were expressed as micromole Trolox equivalent per gram of samples (μmol TE/g) from a Trolox calibration curve (y = 0.0026x + 0.2679).

The FRAP was measured according to the method described by An et al. [2] with some modifications. The working solution was prepared by combining 300 mM acetate buffer (pH 3.6), 20 mM $FeCl_3$, and 10 mM $C_{18}H_{12}N_6$ prepared in 40 mM HCL to a ratio of 10:1:1. Thereafter, 2.4 mL of the working solution was mixed with 0.1 mL of the sample extract and allowed to stand for 30 min at 37 °C before absorbance reading at 593 nm. The results were expressed as micromole Trolox equivalent (μmol TE/g) from a Trolox calibration curve (y = -0.009x + 1.6954).

2.7. FTIR spectral acquisition

The FTIR spectra of samples were obtained using an FTIR spectrometer (Thermo Fisher Scientific Co., ltd., Waltham, MA, USA). The absorbance spectra at 600 – 4000 cm^{-1} were obtained by 32 scans, with a spectral resolution of 2 cm^{-1} and a temperature of 25 °C as outlined by Xu et al. [34].

2.8. Scanning electron microscopy (SEM)

The ultrastructural changes in samples were examined using a scanning electron microscope (Zeiss Merlin Field Emission SEM, Carl Zeiss NTS GmbH, Oberkochen, Germany). Dried red dragon fruit slices were cut into 2 mm × 2 mm × 1.5 mm slices, fixed on the SEM specimen stub, coated with gold, and observed at 100 kPa.

2.9. Statistical analysis

Experimental data were computed and presented as mean values of triplicate data and standard deviations. Results were subjected to analysis of variance (ANOVA) and least significant difference (LSD) post hoc comparison of the means at $p < 0.05$ using Statistix version 9.0 analytical software (Analytical Software ltd., Tallahassee, FL, USA). Pearson's correlation analysis was carried out using OriginPro 9 (Origin Lab., MA, USA) software.

3. Results and discussion

3.1. Effects of pretreatments on drying kinetics

Fig. 1a presents the drying data for RDFS under different pretreatment conditions. The results showed that the moisture ratio declined steadily as drying progressed for all the pretreatment methods, with the drying time ranging from 220 – 300 min. The reductions in moisture content were more rapid for US-FTS, especially US50S, followed by US70S and US25S, with drying times ranging from 220 to 260 min,

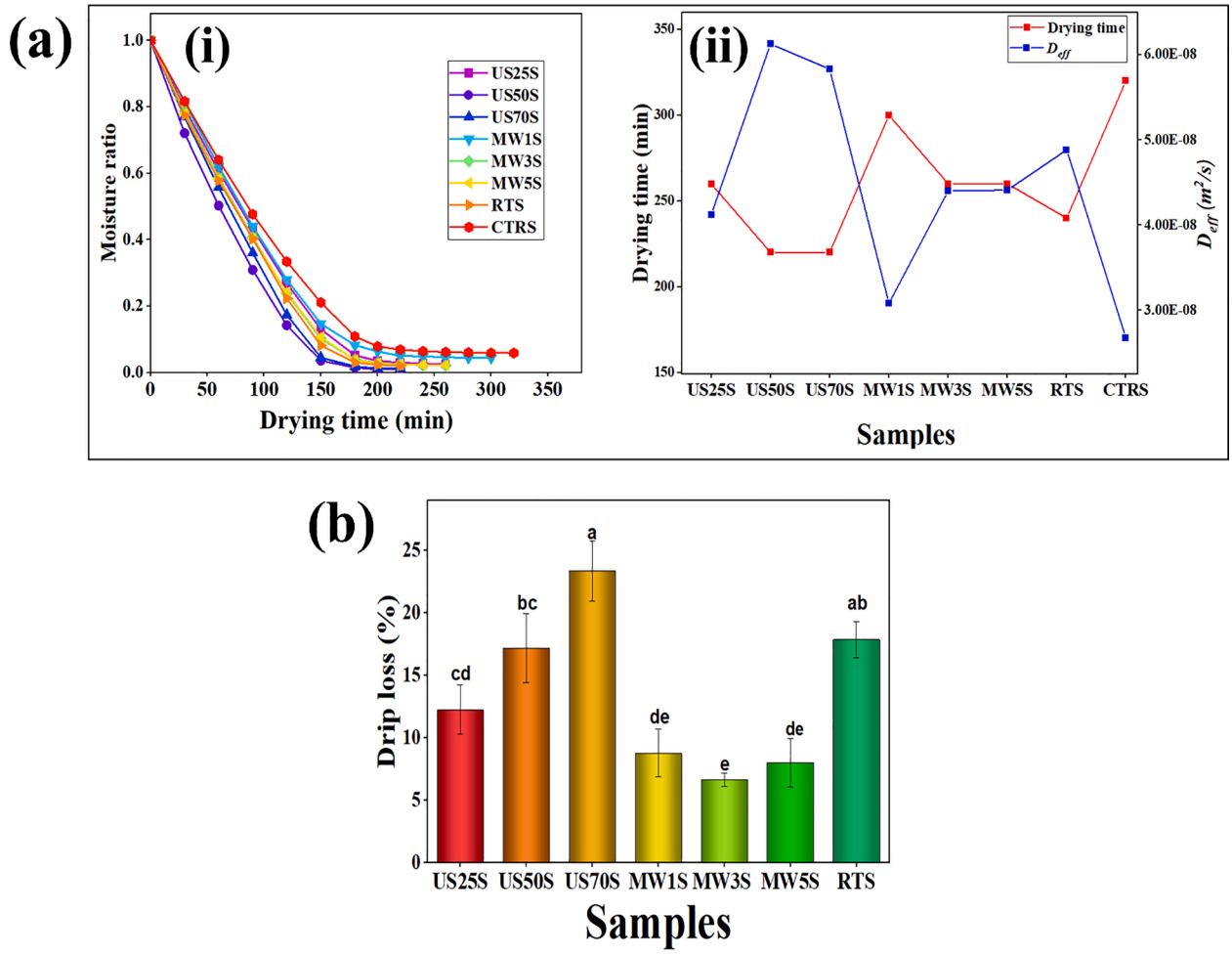

Fig. 1. Effects of thermoultrasound and microwave-assisted freeze–thaw pretreatments on (a) drying kinetics of RDFS during infrared drying: (i) moisture ratio (ii) drying time and moisture diffusivity and (b) drip loss of RDFS. US25S: ultrasound thawing at 25 °C; US50S: ultrasound thawing at 50 °C; US70S: ultrasound thawing at 70 °C; MW1S: microwave thawing at 100 W; MW3S: microwave thawing at 300 W; MW3S: microwave thawing at 500 W; RTS: air thawing at room temperature; CTRS: unpretreated samples.

whereas the decreases in moisture ratio were power-dependent for MW-FTS with drying times in the range of 260 – 300 min. Comparatively, the drying time was higher by up to 8.33 % for US-FTS, and 25 % for MW-FTS in comparison with RTS, with the exception of US50S and US70S, and all pretreatments led to reductions in drying time when compared with CTRS. The observed acceleration in moisture removal for US50S might be related to the combinative effect of temperature and extended acoustic cavitation, which might lead to a critical breakdown of sample tissues, triggering the formation of micropores [9]). The same phenomenon was also been reported by Xu et al. [34], where US-FT resulted in up to 56.25 % reduction in drying time during vacuum freeze-drying of okra. In addition, since the heating process during MW-FT was more pronounced at high power, water evaporation likely occurred during thawing, resulting in lower moisture content and increased drip loss (Fig. 1c). Thus, the conjunctional effect of moisture loss and higher core temperature of the samples resulted in the creation of micro-fissures and subsequent reductions in drying time during IRD, particularly for MW5S [16]. Besides, studies have shown that rapid thawing could impede the structural collapse of samples for minimizing drip loss. Thus, considerable structural damage, high drip loss and the resultant decrease in moisture content caused by slow thawing for RTS might be responsible for the lower drying time when compared with US-FTS and MW-FTS, with the exception of US50S and US70S (Phinney et al., 2017; [18]. Xu et al. [34] also reported a similar reduction in the drying time of RTS in comparison with US-FTS during vacuum freeze-drying of okra. Overall, freeze–thaw pretreatments effectively improved the moisture removal rate, which might be attributed to the formation of ice crystals and the development of micro-fissures on the cell wall of RDFS [18].

3.2. Effects of pretreatments on effective moisture diffusivity (D_{eff})

The D_{eff} of RDFS during IRD drying is shown in Fig. 1b, and the values were within the acceptable range of $10^{-12} - 10^{-8}$ m^2/s obtainable for food materials [5]. Particularly, the values for US-FTS were 4.12×10^{-8}, 6.13×10^{-8}, and 5.83×10^{-8} m^2/s for US25S, US50S, and US70S, respectively, while the D_{eff} increased from 3.08×10^{-8} to 4.41×10^{-8} m^2/s with increasing power for MW-FTS. Compared with RTS, D_{eff} increased for US50S and US70S and decreased for US25S and all MW-FTS, and D_{eff} was higher in pretreated samples, which could be attributed to the creation of intracellular spaces on the sample surface, which facilitated and accelerated the moisture removal rate [18]. In addition, microstructural alterations by US-FT were mainly attributed to the chemical and mechanical effects of cavitation that occurred from the creation, growth, and collapse of bubbles around the surface of the materials, causing the formation of micropores on the thawed sample tissue, for promoting moisture migration during drying [32]. The cavitation effects were more pronounced at higher temperatures and longer treatment durations, hence a higher D_{eff} was obtained for US50S [1,20]. Furthermore, increases in D_{eff} from high-temperature US-FT might be related to the production of high-speed jets around the sample surfaces caused by elevated temperatures, which led to critical damage, loss of turgor pressure of cells, and formation of micro-fissures on samples (Xu et al., 2022). On the other hand, a rapid increase in sample temperature and amplified vapour gradient between the surface and centre of the sample led to higher heating rates, particularly at high power for MW-FTS during IRD [38].

3.3. Effects of pretreatments on physicochemical properties

3.3.1. Colour properties

The changes in colour properties of RDFS during IRD are presented in Table 1. The L^*, a^*, b^*, chroma, and hue of fresh RDFS were 27.98, 27.39, 0.81, 27.41, and 1.68°, respectively. For US-FTS, the highest and lowest values of L^* were observed for US50S and US25S, respectively, and increasing the temperature increased a^* and chroma values to reach a range of 6.67–14.01 and 6.67 – 14.00, respectively. Conversely, the highest and lowest b^* and hue values were observed for US25S and US50S. For MW-FTS, the L^* values ranged from 36.12 – 37.18, and the highest value was observed for MW5S. Increasing the power led to increases in a^* and chroma, with values ranging from 5.38 to 7.88 and 5.39 – 7.89, respectively, while the b* and hue° decreased from 0.31 to 0.13 and 3.35° to 0.92°, respectively, with increasing power. The ΔE, which is an indicator of colour deviation from fresh samples, was within the range of 19.08 – 20.88 for MW-FTS, and the lowest value was obtained for MW3S, followed by MW5S, whereas increasing the temperature increased the values to a range of 20.54 – 24.44 for US-FTS. Compared with RTS, the ΔE was reduced by up to 10.17 % for US25S and 14.52 % for MW-FTS, and compared with CTRS, ΔE was increased by 8.31, 12.16, and 2.43 % for US50S, US70S, and RTS, respectively. The occurrence of enzymatic reactions like non-enzymatic and *Maillard* browning during the drying process is mainly responsible for the changes in the colour of dried products, and these reactions are associated with several factors including treatment time and temperature [13]. In general, the temperature-dependent increase in the ΔE for US-FTS was likely due to the exposure of the samples to elevated temperatures during pretreatments, which resulted in ascorbic acid browning, Maillard reaction, and degradation of betacyanin (Anaya-Esparza et al., 2017). Additionally, lower ΔE for high-power MW-FT might be connected to lower leaching losses and reduced thawing and drying time, which led to the preservation of colour pigments like betacyanin [31,30,22]. Colour pigments are typically susceptible to rapid degradation in the presence of light and oxygen, and exposure to aerobic conditions for an extended duration during RT-FT led to enzymatic browning and consequent increases in ΔE for RTS [19,5].

3.3.2. Rehydration ratio (RR)

As shown in Fig. 2a, pretreatments significantly affected the RR of RDFS. Particularly, the highest and lowest RR values of 3.97 and 3.71

Table 1
Effects of thermoultrasound and microwave-assisted freeze–thaw pretreatments on colour parameters of red dragon fruit slices during infrared drying.

Samples	L^*	a^*	b^*	ΔE	Chroma	Hue (°)
Fresh	27.98 ± 1.12^{c}	27.39 ± 4.16^{a}	0.81 ± 0.20^{a}	–	27.41 ± 4.17^{a}	1.68 ± 0.16^{abc}
US25S	36.36 ± 0.11^{ab}	6.67 ± 0.67^{c}	0.14 ± 0.05^{b}	20.54 ± 0.65^{cd}	6.67 ± 0.66^{c}	1.20 ± 0.52^{bcd}
US50S	37.81 ± 0.44^{a}	12.64 ± 2.04^{b}	-0.86 ± 0.36^{c}	23.60 ± 1.67^{ab}	12.67 ± 2.06^{b}	-3.79 ± 1.03^{f}
US70S	37.28 ± 0.17^{ab}	14.00 ± 0.05^{b}	-0.70 ± 0.17^{c}	24.44 ± 0.10^{a}	14.01 ± 0.06^{b}	-2.87 ± 0.69^{ef}
MW1S	36.27 ± 0.86^{ab}	5.38 ± 0.15^{c}	0.31 ± 0.13^{b}	20.88 ± 0.18^{cd}	5.39 ± 0.15^{c}	3.35 ± 1.44^{a}
MW3S	36.12 ± 0.71^{b}	5.50 ± 0.12^{c}	0.26 ± 0.09^{b}	19.08 ± 0.38^{d}	5.51 ± 0.12^{c}	2.69 ± 0.96^{ab}
MW5S	37.18 ± 0.40^{ab}	7.88 ± 0.32^{c}	-0.13 ± 0.02^{b}	20.05 ± 0.45^{cd}	7.89 ± 0.32^{c}	-0.92 ± 0.12^{de}
RTS	36.98 ± 0.40^{ab}	5.13 ± 0.22^{c}	0.06 ± 0.04^{b}	23.07 ± 0.38^{ab}	5.13 ± 0.22^{c}	0.60 ± 0.42^{bcd}
CTRS	36.73 ± 0.04^{ab}	6.45 ± 0.89^{c}	-0.04 ± 0.01^{b}	21.79 ± 0.78^{bc}	6.45 ± 0.89^{c}	-0.36 ± 0.04^{cd}

Means ± standard deviation ($n = 3$). Different lowercase letters in the same column are significantly different ($p < 0.05$).
US25S: ultrasound thawing at 25 °C; US50S: ultrasound thawing at 50 °C; US70S: ultrasound thawing at 70 °C; MW1S: microwave thawing at 100 W; MW3S: microwave thawing at 300 W; MW5S: microwave thawing at 500 W; RTS: air thawing at room temperature; CTRS: unpretreated samples.

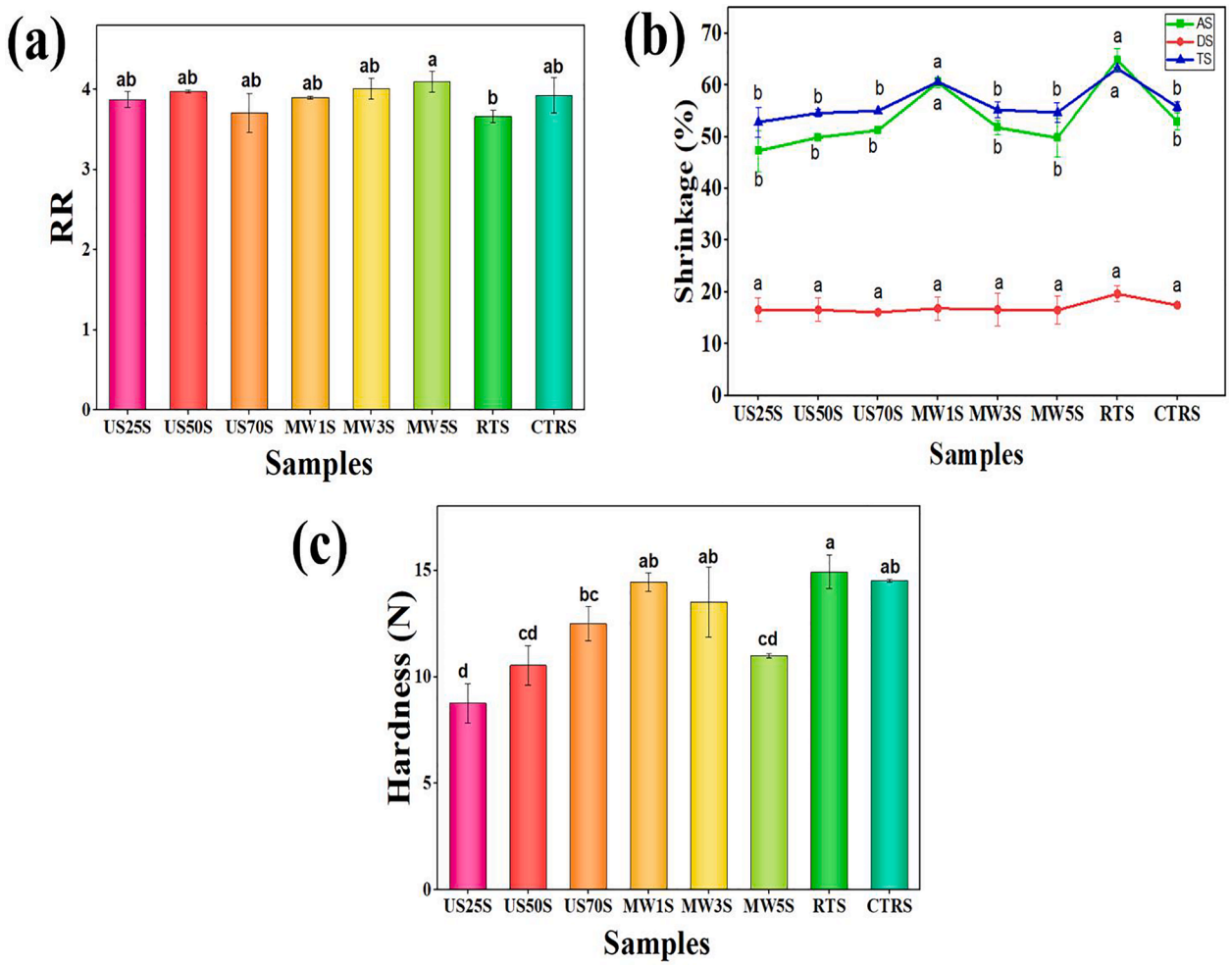

Fig. 2. Effects of thermoultrasound and microwave-assisted freeze–thaw pretreatments on the physicochemical quality of RDFS during infrared drying. (a) RR (b) shrinkage and (c) hardness.

were obtained for US50S and US70S, respectively, for US-FTS, and increasing the power led to increases in RR to a range of 3.90–4.10 for MW-FTS. In contrast, compared with the RTS value of 3.66, MW-FT and US-FT treatments increased RR and compared with the CTRS value of 3.92, US50S, MW3S, and MW5S presented higher values. Localized overheating has been reported during ultrasound treatments, and the temperature rise intensifies cavitation. The combination of high temperatures and prolonged exposure to acoustic waves caused substantial damage to cells, hence the inability of capillaries and cavities to absorb moisture, especially for US50S [20]. Meanwhile, the observed increases in RR at higher power for MW-FTS could be due to water retention in intercellular gaps created on cell tissues by high energy release during thawing (Horuz et al., 2017). The significant increases in RR for US-FT and MW-FT pretreatments might be resulted from the better preservation of sample structure by reduced thawing time. On the other hand, lower leaching losses and thawing time, and reduced breakdown of cell walls during MW-FT impeded excessive structural damage and consequently improved water absorption when compared with US-FT and RT-FT [30].

3.3.3. Degree of shrinkage

The degree of shrinkage in RDFS is presented in Fig. 2b, and the results revealed that increasing the temperature increased TS and AS and decreased DS for the US-FTS, while increasing the power during MW-FT reduced TS, DS and AS from 60.48 to 49.80 %, 16.85 to 16.51 %, and 60.02 to 49.89 %, respectively. The results also demonstrated that US-FT and MW-FT pretreatments were more effective for minimizing shrinkage in comparison with RT-FT, and when compared with CTRS, higher overall shrinkages were observed for MW1S and RTS. Depending on the thawing rate, additional tissue damages can occur during the thawing process, and rapid thawing tends to improve the preservation of cell structure, while slow thawing could be potentially more destructive when compared with the freezing process [12]. The osmotic gradient caused by the low osmotic pressure of the extracellular fluid during the slow thawing process allows for vast water migration into the cell of food tissue, causing it to swell and rupture. This rupturing might be responsible for the collapse of cell structure and the accompanying shrinkages observed for the slow-thawed samples [12]. Some studies have suggested that rapid moisture removal rates led to higher moisture gradients and consequent increases in sample shrinkages. Hence, the rapid moisture removal rates caused by high-temperature acoustic cavitation might be responsible for the higher shrinkages observed for US-FTS [23]. Likewise, accelerated moisture removal combined with severe structural damage to the cell wall during RT-FT might be responsible for increased shrinkages for RTS [23]. Besides, increasing the power intensified heat generation within the food and increased the pressure difference between the core and surface of samples, resulting in rapid mass transfer and reduced shrinkage during thawing and subsequent drying for MW-FTS (Kumar et al., 2018).

3.3.4. Texture

The effects of pretreatments on the hardness of RDFS are presented in

Fig. 2c, and the results showed that the hardness of the US-FTS ranged from 8.77 to 12.50 N, with the highest and lowest values observed for US70S and US50S, respectively, while the hardness of MW-FTS ranged from 10.99 to 14.46 N, with MW5S presenting the lowest value, followed by MW1S. Decreases in hardness were observed for US-FTS and MW-FTS when compared with RTS and CTRS. Lower hardness at low temperatures for UT-FTS might be attributed to significant deformation in the duct structure of the cell as a result of intensified electroporation phenomenon from longer exposure time [33]. Meanwhile, the rupture and disintegration of the cell structure by the increasing pressure gradient between the interior of the samples and surface at high temperatures for MW-FTS resulted in the compromise of structural integrity, and consequent reductions in drying time, leading to tensile stress and reduced thickness shrinkage, which was linked with a reduced hardness of dried products (Kim et al., 2011; Kumar et al., 2018). There was also a significant correlation between shrinkage and texture of samples, which was in agreement with reports that a high shrinkage rate led to increases in the density of samples and subsequent increases in their hardness [24,35,33].

3.4. Effects of pretreatments on phytochemical composition and antioxidant activities

3.4.1. Total phenolic contents (TPC) and total flavonoid contents (TFC)

The effects of pretreatments on the TPC and TFC of RDFS are summarized in Fig. 3a and 3b. The TPC and TFC of fresh RDFS were 55.63 mg GAE/100 g and 95.75 mg QUE/100 g, respectively, and IRD led to their significant increases in TPC and TFC. For US-FTS, the highest and lowest values of 116.71 and 97.76 mg GAE/100 g were observed for US25S and US50S, respectively, while the highest and lowest TPC values of 109.39 and 106.60 mg GAE/100 g were observed for MW3S and MW1S, respectively, for MW-FTS. Compared with 114.14 and 115.21 mg GAE/100 g for RTS and CTRS, respectively, lower TPC values were observed for all pretreatments, with the exception of 116.71, and 115.94 mg GAE/100 g for US25S and US70S, respectively. Likewise, US70S and US50S presented the highest and lowest values of 323.25 and 249.50 mg QUE/100 g, respectively, for US-FTS, while the highest and lowest TFC values of 316.58 and 279.50 mg QUE/100 g were observed for MW1S and MW3S, respectively, for MW-FTS. In addition, RTS had the highest overall TFC value of 329.50 mg QUE/100 g and compared with CTRS value of 296.58 mg QUE/100 g, pretreatments led to increases in TFC with the exception of 249.5 and 279.7 mg QUE/100 g for US50S and MW300S, respectively. The improved retention of TPC observed for US25S might be attributed to the enhanced release of bound phenolic caused by substantial disruption of the cell wall during cavitation, while the increase in TPC for MW3S might be due to reduced leaching loss and drying time [28].

On the other hand, extended thawing duration and high temperatures increased oxidative reactions, which resulted in the breakdown of TPC into various byproducts for increasing the production of free hydroxyl radical species, leading to the degradation of phenolics and flavonoids compounds in US50S [17]. The observed increases in the TPC for US-FTS were probably due to the ability of ultrasonic cavitation to weaken the bond of cell wall phenolic compounds, thereby aiding their release and extraction [28,32]. Additionally, exposure of samples to thermo-ultrasonic acoustic cavitation for an extended duration might intensify the damage and breakdown of cells and the release of flavonoid compounds into the exudate during thawing, leading to the lower retention of TFC in US50S. In a similar study, US-FT presented better TPC retention when compared with RT-FT during vacuum freeze-drying of okra, due to the inhibition of oxidative degradation of phenolic compounds by reductions in dissolved oxygen present in sample tissues [33]. In addition, although shortened thawing time was associated with MW-FTS, the better-preserved sample structure, evident from the microstructural observation, might impede the catabolization of phenolic components during drying and limit its bio-accessibility for

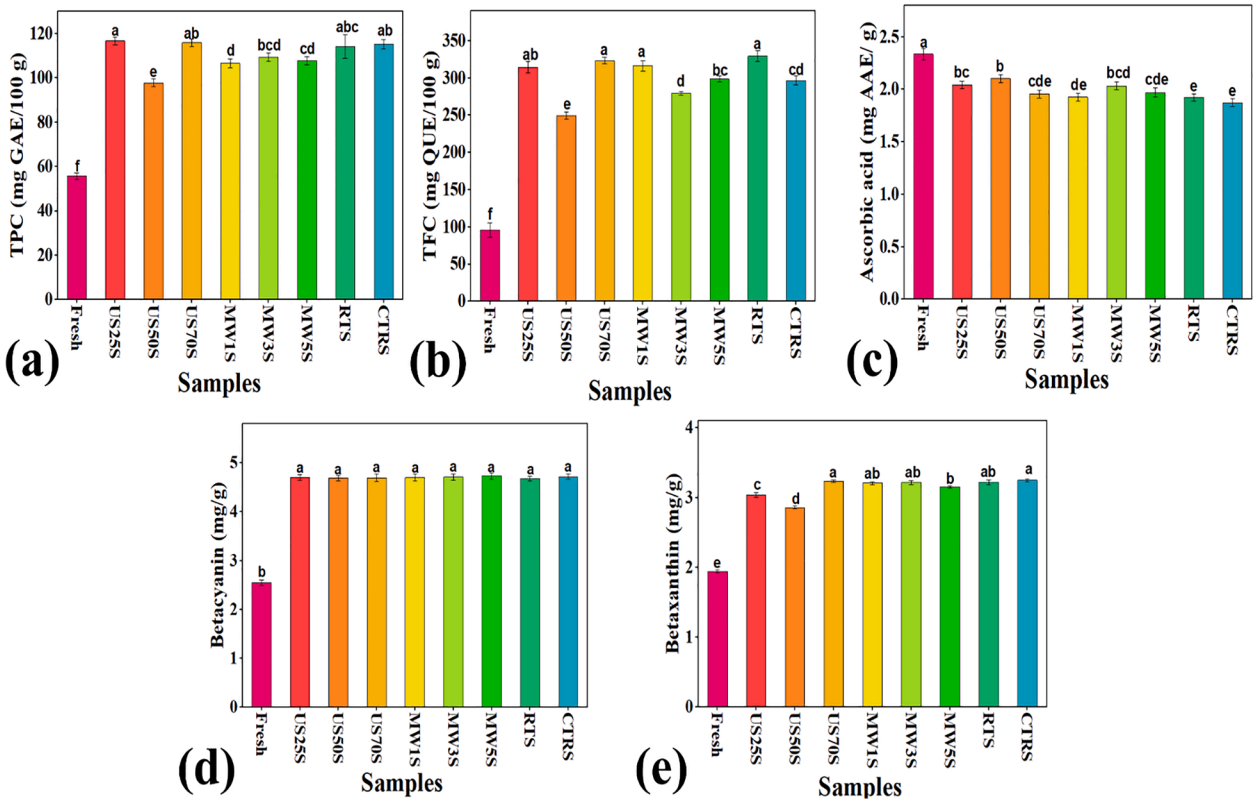

Fig. 3. Effects thermoultrasound and microwave-assisted freeze–thaw pretreatments on the phytochemical composition of RDFS during infrared drying. (a) TPC (b) TFC (c) ascorbic acid (d) betacyanin and (e) betaxanthin.

MW-FTS. Furthermore, the increase in TFC for MW1S could be explained by several factors, such as the reduced heating intensity during low-power MW-FT pretreatments and limited oxidation reactions induced by the non-porous nature of MW1S [40].

3.4.2. Ascorbic acid content (AAC)

The AAC of fresh RDFS was 2.34 mg/g (Fig. 3c) and drying led to losses in AAC, and in particular, the highest and lowest values of 2.10 and 1.95 mg/g were observed for US50S and US70S, respectively, among US-FTS, while MW3S and MW1S presented the highest and lowest values of 2.03 and 1.93 mg/g, respectively, among MW-FTS. Compared with RTS and CTRS, US-FTS and MW-FTS presented higher AAC, indicating the promising potential of the pretreatments for improving AAC retention. Ascorbic acid is thermosensitive and the losses observed during IRD might be associated with the exposure of samples to elevated temperatures [33]. Meanwhile, the improved retention of AAC for UT-FTS and MW-FTS might be linked to several factors, including reduced thawing and drying time, minimal leaching losses, and enhanced cellular catabolism [36]. Also, ascorbic acid is easily decomposed at high temperatures and prolonged exposure to thermo-ultrasonic cavitation might disrupt the natural liquid around the boundary phase, destroying the cellular structure to cause the release of cellular content into the surrounding liquid, hence, US-FT at high temperature was not favourable for AAC retention [8,34]. Although there are no studies on US-FT pretreatments in relation to drying, Cheng et al. [8] observed that increasing the temperature reduced the AAC of edamame during ultrasound thawing. Besides, the better preservation of AAC for MW3S was probably due to the combinative effects of reduced thawing time, leaching loss, drying time and thermal effects at lower microwave radiative powers [31]. Improved retention of AAC by MW-FT treatment at 300 W, attributed to rapid thawing and reduced exposure of samples to oxygen has also been reported for frozen-thawed mango [22].

3.4.3. Betalain contents

The effects of pretreatments on the betalain composition of RDFS are shown in Fig. 3d and Fig. 3e. The betacyanin and betaxanthin contents of fresh RDFS were 2.55 and 1.94 mg/g, respectively, and increased for all dried samples. The betalain contents of the US-FTS were in the range of 4.69–4.70 mg/g and 2.86–3.24 mg/g, respectively, and the highest and lowest values were observed for US25S and US50S, and US70S and US50S for betacyanin and betaxanthin respectively. For MW-FTS, the betacyanin content increased from 4.70 to 4.73 mg/g with increasing power, while the highest (3.22 mg/g) and lowest (3.16 mg/g) values of betaxanthin were observed for MW3S and MW5S, respectively. Comparatively, US-FTS and MW-FTS presented better betacyanin contents when compared with RTS, and with exception of MW3S, pretreatments were ineffective for retaining the betacyanin contents when compared with CTRS value of 4.72 mg/g. On the other hand, with the exception of US70S, betaxanthin content was lower for US-FTS and MW-FTS when compared with RTS, and pretreatments characteristically reduced betaxanthin content when compared with CTRS value of 3.25 mg/g.

The increase in betaxanthin for US70S might be related to the catabolization and cavitation effect of thermo-ultrasonic waves and consequent release of betalain molecules and reductions in thawing and drying times, while the better retention of betaxanthin for MW3S might be attributed to lower drip loss. In addition, lower betacyanin and betaxanthin contents for US50S were likely connected with the greater destruction of the cellular structure caused by high temperature and extended exposure, which led to increased leaching loss of betalain compounds and formation of high concentration of hydroxyl radicals (Cheng et al., 2013). Moreover, lower values of betacyanin for RTS were due to the mechanical disruption of the cell wall and consequent porous nature of RTS, which led to higher leaching loss and intensification of heat damage to betacyanin molecules [21]. Furthermore, loss of colour pigments by leaching and oxidative reactions induced by exposure of samples to oxygen and heat during pretreatments might have resulted in the reduced retention of betaxanthin molecules for pretreated samples (Vallespir et al., 2018b).

3.4.4. Antioxidant activities

The antioxidant activity of RDFS expressed in terms of ABTS, HRSA, CUPRAC, and FRAP are presented in Fig. 4. Fresh RDFS presented ABTS, HRSA, CUPRAC, and FRAP values of 21.07 μmol TE/g, 32.56 %, 138.02 μmol TE/g, and 26.19 μmol TE/g, respectively, and drying led to increases in antioxidant activity due to the increased retention of phytochemical compounds in dried samples. However, ABTS increased to values of 27.08, 26.94, and 26.97 μmol TE/g, respectively, were observed for US25S, US50S, and US70S (Fig. 4a), while increasing the power led to decreases in ABTS to a range of 27.47 – 26.97 μmol TE/g for MW-FTS. Comparatively, UT-FTS and MW-FTS presented higher ABTS values in comparison with RT-FTS, and with the exception of RTS, pretreatments were effective for enhancing the ABTS activity when compared with CTRS values of 26.79 μmol TE/g. For HRSA, increasing the temperature significantly decreased HRSA from 81.91 to 69.72 % for US-FTS (Fig. 4b), and the highest and lowest values of 76.88 and 69.69 % were observed for MW3S and MW1S, respectively, for MW-FTS. Compared with RTS, MW1S presented lower values, followed by US70S, and pretreatments were effective for enhancing HRSA when compared with CTRS. For CUPRAC, increasing the temperature increased the values from 378.26 to 398.75 μmol TE/g with the exception of US50S (Fig. 4c) for US-FTS, and for MW-FTS, increasing the microwave power reduced the values from 373.24 to 349.88 μmol TE/g. Among the pretreated samples, RTS presented the highest value of 420.671 μmol TE/g, and with the exception of US70S and RTS, pretreatments were ineffective for enhancing CUPRAC when compared with CTRS value of 392.98 μmol TE/g. In addition, the FRAP increased to37.64, 34.00, and 39.65 μmol TE/g for US25S, US50S and US70S, and 37.91, 36.76, and 37.17 μmol TE/g for MW1S, MW3S, and MW5S, respectively, but, US-FTS and MW-FTS presented lower FRAP values in comparison with RTS and CTRS (Fig. 4d).

The improved ABTS result for US25S was consistent with the improved retention of TPC and likely connected to the lower drip loss and breaking of covalent and ionic bonds between the phenolic compounds and cell walls [15]. In addition, hydroxylated derivatives were reported to enhance antioxidant activities produced during ultrasound treatments, and these derivatives could also contribute to the increase in ABTS during IRD, especially for US25S [4,33]. Similar increases in ABTS by UT-FT have been reported for okra during vacuum freeze-drying [34]. The antioxidant potential of foods is usually associated with the antioxidant properties of their constituent phytochemicals like flavonoids, tannins, phenolic acids, and belatains, hence, the increases for MW3S might be connected with the better preservation of heat-labile phenolic and flavonoid compounds by lower radiative energy during thawing [15]. More so, the power-dependent increases in ABTS for MW-FTS might be related to the leaching of phytochemicals caused by increased catabolization of biomolecules at high-power MW-FT treatments. In addition, lower ABTS obtained for RT-FTS might be related to the prolonged thawing time associated with RT-FT, which led to the exposure of samples to prolonged aerobic conditions and oxidative decompositions of phytochemicals with antioxidant potentials [31].

Furthermore, the combined effects of reduced thawing time and limited radiation impingement on samples during thawing were likely responsible for the preservation of phytochemicals like ascorbic acid and betaxanthin, which correspondingly improved HRSA [15]. On the other hand, high-temperature US-FT might cause catabolism of biomacromolecules by cavitation, leading to their losses by leaching [8]. The results also indicated that the application of low-temperature US-FT and moderate-power MW-FT pretreatment was favourable for improving the HRSA during IRD. Additionally, high CUPRAC and FRAP activity for US70S might be attributed to the reduced drying time from

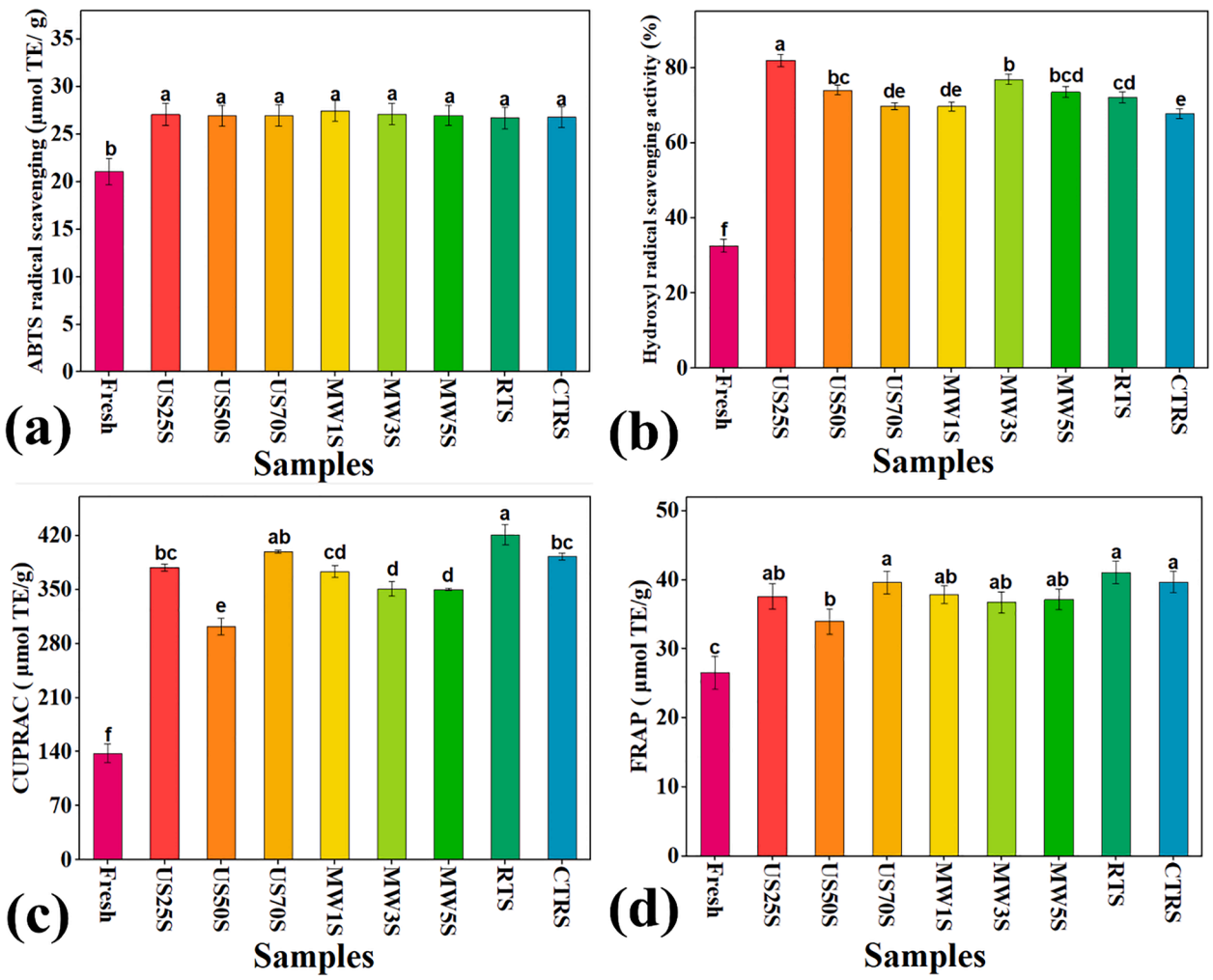

Fig. 4. Effects of thermoultrasound and microwave-assisted freeze–thaw pretreatments on antioxidant activity of RDFS during infrared drying. (a) ABTS radical scavenging (b) hydroxyl radical scavenging activity (c) CUPRAC and (d) FRAP.

microstructural modifications and shorter thawing time, which minimized the degradation effect of US-FT on betaxanthin and flavonoids [2,34]. Asides from the thermal degradation of heat-labile biomacromolecules, US-FT and MW-FT pretreatments might disrupt covalent bonds to release bound phytochemicals into the fluid, which could not be reabsorbed by the cells during thawing. The loss of phytochemicals by leaching for US-FTS and MW-FTS might account for the lower CUPRAC and FRAP when compared with RTS [30].

3.5. Effects of pretreatments on functional groups

The effects of pretreatments on functional groups can be evaluated by analyzing FTIR spectra of RDFS and results are shown in Fig. 5a, which presented structural similarities with characteristics of strong bands of the hydroxyl group around 3200–3600 cm^{-1}, and distinct peaks at 3315 – 3308 cm^{-1}. The specific peaks around 2926–2925 cm^{-1} were representative of the asymmetric C—H stretch and the strong peaks at 1640–1621 cm^{-1} typically indicated the asymmetric C═O stretch of COO, which was representative of the presence of uronic acid. Furthermore, C—H or O—H bending vibrations were associated with the 1417 cm^{-1} band, and distinct peaks were observed at 1417 – 1416 cm^{-1}, indicating the presence of nitrogen-containing functional groups, confirming the presence of betalain compounds in RDFS. Minor peaks between 1058 and 1398 cm^{-1} were characteristic overtone bands of O—H and C—H, which indicated the presence of multiple forms of carbohydrates such as pectin, hemicellulose, and lignin. In addition, the peaks at 1047 – 1046 cm^{-1} represented C—O broadening, signifying the presence of phenols. This was because the C—O stretches of alcohol and phenol usually form a strong band in the range of 1300 to 1000 cm^{-1}. Overall, spectral results showed that the structural changes caused by the pretreatment resulted in a slight shift in spectral peaks, revealing related differences in the phytochemical properties of RDFS [10,34].

3.6. Effects of pretreatments on microstructure

The microstructure of RDFS indicated that the cell wall degradation was less severe for CTRS, resulting in a smooth structure with fewer cavities, and was markedly different for the pretreatments and depended on the method employed (Fig. 5b). the cell structure became more porous with increasing temperature for US-FTS, probably due to high temperature-induced intensification of acoustic cavitation and sponge effects. Similar microstructural alterations by US-FT were also reported for okra during vacuum freeze-drying [34]. On the other hand, MW1S displayed a smooth and compact structure when compared with MW3S and MW5S, which presented visible intracellular spaces from the formation of micro-fissures on surfaces of the tissues due to the collapse and expansion of the sample matrix from increased heat transfer [5]. Compared with the MW-FTS and CTRS, the fissures for RT-FTS were substantially larger and detached, which might be resulted from the extended thawing duration that might lead to the collapse and damage of organelles and consequent compromise of structural integrity (Vallespir et al., 2018a). Conversely, cell wall degradation was less severe for

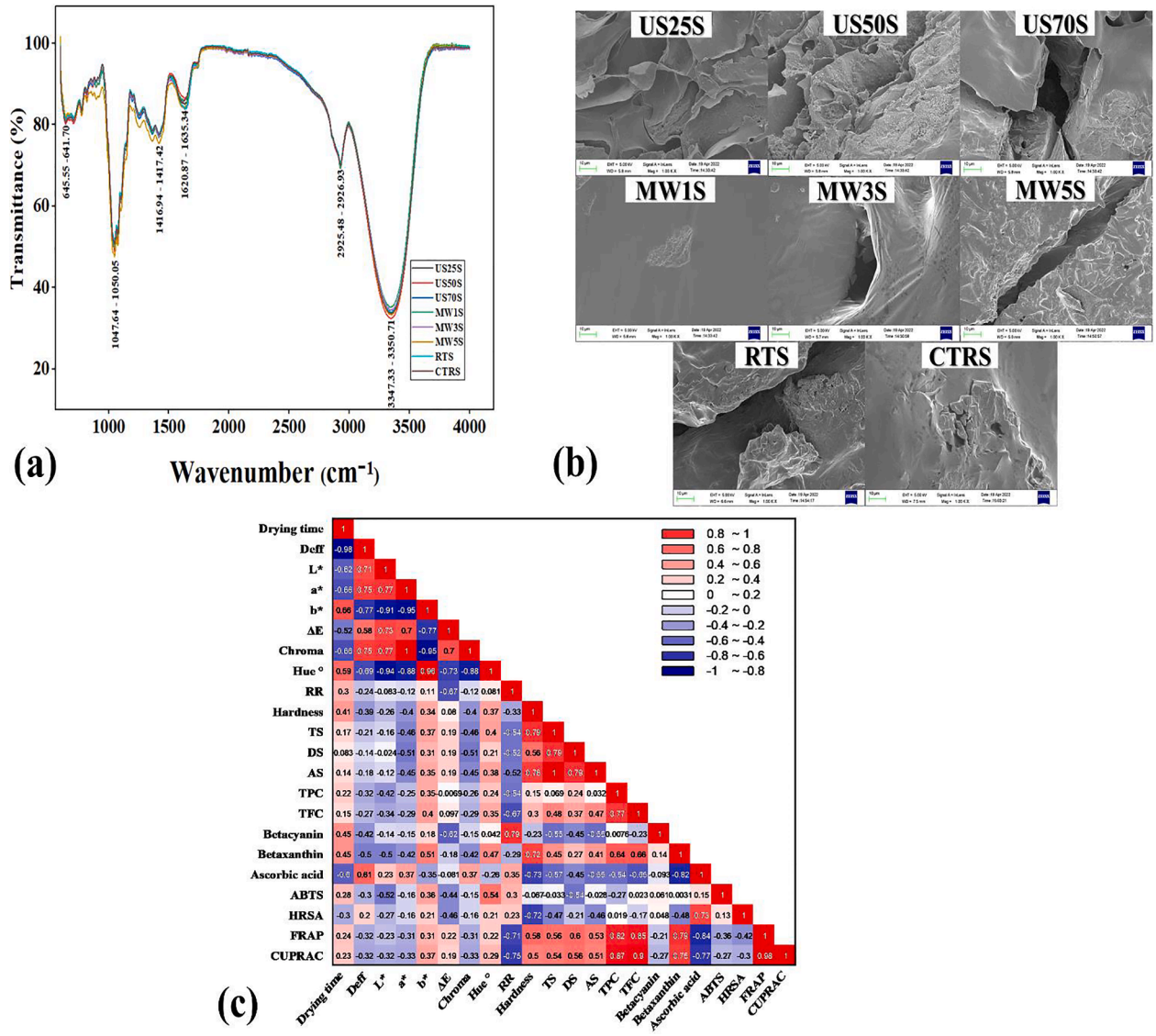

Fig. 5. Effects of thermoultrasound and microwave-assisted freeze–thaw pretreatments on (a) FTIR spectra (b) microstructure and (c) Pearson's correlation matrix of RDFS during infrared drying.

CTRS, resulting in a smooth structure with fewer cavities. Overall, the resultant microstructural alterations impacted the mass transfer, structure, and accessibility of biomolecules, and similar microstructural changes from US-FT and RT-FT pretreatments have been reported for okra and lotus roots during vacuum freeze-drying and IRD-convective drying [34,36].

3.7. Pearson's correlation analysis

Pearson's correlation analysis was employed for analyzing the relationship between the quality properties as shown in Fig. 5c. The results indicated that D_{eff} showed a significant ($p < 0.05$) positive correlation with L^* (r = 0.71, a^* (r = 0.75) and chroma (r = 0.75). The L^* also showed a significant positive relationship with chroma (r = 0.77), a^* (r = 0.77) and ΔE (r = 0.73), while a^* and chroma (r = 1, $p < 0.05$), and b^* and hue (r = 0.96, $p < 0.05$) were also positively correlated. The correlation analysis results also revealed significant positive relationship between RR and betacyanin (r = 0.79, $p < 0.05$), and the hardness exhibited significant positive correlations with shrinkage (r = 0.76) and betaxanthin (r = 0.72). Similarly, TPC showed significant positive correlations with TFC (r = 0.77), FRAP (r = 0.82), and CUPRAC (r = 0.87), while TFC was positively correlated with FRAP (r = 0.85) and CUPRAC (r = 0.9). Furthermore, there was also a significant relationship between AAC and HRSA (r = 0.73), and betaxanthin showed a significant positive correlation with FRAP (r = 0.79) and CUPRAC (r = 0.75). Overall, the above results should be sufficient to conclude that phytochemicals contributed significantly to the antioxidant activity of RDFS and could be linked to a wide range of chemical reactions induced during freeze–thaw pretreatments and infrared drying of RDFS.

4. Conclusions

The current study showed that thermoultrasound and microwave -assisted freeze–thaw (US-FT and MW-FT) pretreatments led to ice crystal formation and subsequent creation of intracellular fissures to varying extents during thawing, and consequently impacted the infrared drying of RDFS. These ultrastructural alterations facilitated moisture migration to enhance D_{eff} and reduce the drying time of RDFS, especially for US-FT pretreatments. Pretreatments also caused irreversible structural alterations and induced chemical changes that influenced the physicochemical quality and phytochemical compositions. Low-temperature US-FT pretreatments were favourable for improving

physicochemical and bioactive properties, with the exception of TFC, FRAP, and CUPRAC, which were better preserved by high-temperature US-FT pretreatments, while high-power MW-FT improved physicochemical qualities and low-power MW-FT caused increases in phytochemicals and antioxidant activities. Collectively, US-FT presented overall enhancements in the quality of RDFS, RT-FT ensured better retention of TFC, consequently increasing FRAP and CUPRAC, while pretreatments were not favourable for betaxanthin retention. The results further indicated that the improved thawing methods and conditions could ameliorate critical cell damage caused by freezing, thus, providing fundamental background for the augmentation of freeze–thaw pretreatments for infrared drying of biological materials. However, further studies are required to validate these findings, and optimization studies are also essential for further improving the pretreatment conditions to obtain even better drying efficiency and quality of final products.

CRediT authorship contribution statement

Edidiong Joseph Bassey: Writing – original draft, Formal analysis, Investigation. **Jun-Hu Cheng:** Validation, Funding acquisition, Resources. **Da-Wen Sun:** Supervision, Funding acquisition, Resources, Writing – review & editing.

Declaration of Competing Interest

The authors declare that they have no known competing financial interests or personal relationships that could have appeared to influence the work reported in this paper.

Data availability

Data are available within the article

Acknowledgements

The authors are grateful to the National Natural Science Foundation of China (31972205) for its support. This research was also supported by the International S&T Cooperation Projects of Guangdong Province (2020A0505100007), Guangdong Basic and Applied Basic Research Foundation (2021A1515010644, 2021A1515110396), the Contemporary International Collaborative Research Centre of Guangdong Province on Food Innovative Processing and Intelligent Control (2019A050519001), the Science and Technology Plan Projects of Guangzhou City (202102100009) and the Common Technical Innovation Team of Guangdong Province on Preservation and Logistics of Agricultural Products (2022KJ101). In addition, Bassey Edidiong Joseph is in receipt of a PhD scholarship (2019ZFY014378) from the China Scholarship Council

References

[1] E.M. Alexandre, D.M. Santos-Pedro, T.R. Brandão, C.L. Silva, Study on thermosonication and ultraviolet radiation processes as an alternative to blanching for some fruits and vegetables, Food Bioprocess Technol. 4 (6) (2011) 1012–1019.
[2] K. An, D. Zhao, Z. Wang, J. Wu, Y. Xu, G. Xiao, Comparison of different drying methods on Chinese ginger (*Zingiber officinale Roscoe*): Changes in volatiles, chemical profile, antioxidant properties, and microstructure, Food Chem. 197 (2016) 1292–1300.
[4] M. Ashokkumar, D. Sunartio, S. Kentish, R. Mawson, L. Simons, K. Vilkhu, C. K. Versteeg, Modification of food ingredients by ultrasound to improve functionality: A preliminary study on a model system, Innov. Food Sci. Emerg. Technol. 9 (2) (2008) 155–160.
[5] E.J. Bassey, J.-H. Cheng, D.-W. Sun, Improving drying kinetics, physicochemical properties and bioactive compounds of red dragon fruit (*hylocereus species*) by novel infrared drying, Food Chem. 131886 (2022).
[6] L. Cai, W. Zhang, A. Cao, M. Cao, J. Li, Effects of ultrasonics combined with far infrared or microwave thawing on protein denaturation and moisture migration of Sciaenops ocellatus (red drum), Ultrason. Sonochem. 55 (2019) 96–104.
[7] M. Cao, A. Cao, J. Wang, L. Cai, J. Regenstein, Y. Ruan, X. Li, Effect of magnetic nanoparticles plus microwave or far-infrared thawing on protein conformation changes and moisture migration of red seabream (*Pagrus Major*) fillets, Food Chem. 266 (2018) 498–507.
[8] X.F. Cheng, M. Zhang, B. Adhikari, Effects of ultrasound-assisted thawing on the quality of edamames (*Glycine max (L.) Merrill*) frozen using different freezing methods, Food Sci. Biotechnol. 23 (4) (2014) 1095–1102.
[9] Y. Feng, X. Yu, A.E.A. Yagoub, B. Xu, B. Wu, L. Zhang, C. Zhou, Vacuum pretreatment coupled to ultrasound assisted osmotic dehydration as a novel method for garlic slices dehydration, Ultrason. Sonochem. 50 (2019) 363–372.
[10] Y. Feng, C. Ping Tan, C. Zhou, A.E.G.A. Yagoub, B. Xu, Y. Sun, H. Ma, X. Xu, X. Yu, Effect of freeze-thaw cycles pretreatment on the vacuum freeze-drying process and physicochemical properties of the dried garlic slices, Food Chem. 324 (2020), 126883.
[11] Y. Guo, B. Wu, X. Guo, F. Ding, Z. Pan, H. Ma, Effects of power ultrasound enhancement on infrared drying of carrot slices: Moisture migration and quality characterizations, LWT-Food Sci. Technol. 126 (2020), 109312.
[12] W.R. Jarnagin, P.J. Allen, W.C. Chapman, M.I. D'Angelica, R.P. DeMatteo, R.K. G. Do, J.-N. Vauthey, L.H. Blumgart, Blumgart's Surgery of the Liver, Biliary Tract and Pancreas, sixth ed., Elsevier Inc, Philadelphia, PA, 2017.
[13] S. Kayacan, S. Karasu, P.K. Akman, H. Goktas, I. Doymaz, O. Sagdic, Effect of different drying methods on total bioactive compounds, phenolic profile, in vitro bio accessibility of phenolic and HMF formation of persimmon, LWT- Food Sci. Technol. 118 (2020), 108830.
[15] T.L. Le, N. Huynh, P. Quintela-Alonso, Dragon fruit: A review of health benefits and nutrients and its sustainable development under climate changes in Vietnam, Czech J. Food Sci. 39 (2) (2021) 71–94.
[16] H. Liu, H. Liu, H. Liu, X. Zhang, Q. Hong, W. Chen, X. Zeng, Microwave drying characteristics and drying quality analysis of corn in china, Processes 9 (9) (2021) 1511.
[17] Y. Liu, S. Chen, Y. Pu, A.I. Muhammad, M. Hang, D. Liu, T. Ye, Ultrasound-assisted thawing of mango pulp: Effect on thawing rate, sensory, and nutritional properties, Food Chem. 286 (2019) 576–583.
[18] Z.L. Liu, I. Staniszewska, D. Zielinska, Y.H. Zhou, K.W. Nowak, H.W. Xiao, Z. Pan, M. Zielinska, Combined hot air and microwave-vacuum drying of cranberries: effects of pretreatments and pulsed vacuum osmotic dehydration on drying kinetics and physicochemical properties, Food Bioprocess Technol. 13 (10) (2020) 1848–1856.
[19] S. Manchali, K.N.C. Murthy, S. Nagaraju, B. Neelwarne, Stability of betalain pigments of red beet, in: B. Neelwarne (Ed.), Red Beet Biotechnology, 2013, pp. 55–74.
[20] K.J. Mothibe, M. Zhang, A.S. Mujumdar, Y.C. Wang, X. Cheng, Effects of ultrasound and microwave pretreatments of apple before spouted bed drying on rate of dehydration and physical properties, Drying Technol. 32 (15) (2014) 1848–1856.
[21] O.V. Nistor, L. Seremet, D.G. Andronoiu, L. Rudi, E. Botez, Influence of different drying methods on the physicochemical properties of red beetroot (*Beta vulgaris L. var. Cylindra*), Food Chem. 236 (2017) 59–67.
[22] Y. Peng, J. Zhao, X. Wen, Y. Ni, The comparison of microwave thawing and ultra-high-pressure thawing on the quality characteristics of frozen mango, Foods 11 (7) (2022) 1048.
[23] Z. Ren, X. Yu, A.E.G.A. Yagoub, O.A. Fakayode, H. Ma, Y. Sun, C. Zhou, Combinative effect of cutting orientation and drying techniques (hot air, vacuum, freeze and catalytic infrared drying) on the physicochemical properties of ginger (*Zingiber officinale Roscoe*), LWT-Food Sci. Technol. 144 (2021), 111238.
[24] S.K. Saha, S. Dey, R. Chakraborty, Effect of microwave power on drying kinetics, structure, color, and antioxidant activities of corncob, J. Food Process Eng 42 (4) (2019) e13021.
[25] T. Seerangurayar, A.M. Al-Ismaili, L.J. Jeewantha, A. Al-Nabhani, Experimental investigation of shrinkage and microstructural properties of date fruits at three solar drying methods, Sol. Energy 180 (2019) 445–455.
[28] F. Vallespir, Ó. Rodríguez, V.S. Eim, C. Rosselló, S. Simal, Effects of freezing treatments before convective drying on quality parameters: Vegetables with different microstructures, J. Food Eng. 249 (2019) 15–24.
[29] B. Wang, X. Du, B. Kong, Q. Liu, F. Li, N. Pan, X. Xia, D. Zhang, Effect of ultrasound thawing, vacuum thawing, and microwave thawing on gelling properties of protein from porcine longissimus dorsi, Ultrason. Sonochem. 64 (2020), 104860.
[30] T. Watanabe, Y. Ando, Evaluation of heating uniformity and quality attributes during vacuum microwave thawing of frozen apples, *LWT*- Food Sci. Technol. 150 (2021), 111997.
[31] X. Wen, R. Hu, J.H. Zhao, Y. Peng, Y.Y. Ni, Evaluation of the effects of different thawing methods on texture, colour and ascorbic acid retention of frozen hami melon (*Cucumis melo var. saccharinus*), Int. J. Food Sci. Technol. 50 (5) (2015) 1116–1122.
[32] B. Xu, A. Ren, J. Chen, H. Li, B. Wei, J. Wang, S.M.R. Azam, B. Bhandari, C. Zhou, H. Ma, Effect of multi-mode dual-frequency ultrasound irradiation on the degradation of waxy corn starch in a gelatinized state, Food Hydrocolloids 113 (2021), 106440.
[33] B. Xu, J. Chen, E.S. Tiliwa, W. Yan, S.R. Azam, J. Yuan, B. Wei, C. Zhou, H. Ma, Effect of multi-mode dual-frequency ultrasound pretreatment on the vacuum freeze-drying process and quality attributes of the strawberry slices, Ultrason. Sonochem. 78 (2021), 105714.
[34] X. Xu, L. Zhang, Y. Feng, C. Zhou, A.E.A. Yagoub, H. Wahia, M. Haile, Z. Jin, Y. Sun, Ultrasound freeze-thawing style pretreatment to improve the efficiency of the vacuum freeze-drying of okra (*Abelmoschus esculentus (L.) Moench*) and the quality characteristics of the dried product, Ultrason. Sonochem. 70 (2021), 105300.

[35] S. Yang, S. Jeong, S. Lee, Elucidation of rheological properties and baking performance of frozen doughs under different thawing conditions, J. Food Eng. 284 (2020), 110084.
[36] L. Zhang, X. Yu, S.M. Arun, C. Zhou, Effect of freeze-thaw pretreatment combined with variable temperature on infrared and convection drying of lotus root, LWT-Food Sci. Technol. 154 (2022), 112804.
[37] M. Zhang, B. Bhandari, Z. Fang, Handbook of Drying Of Vegetables And Vegetable Products, CRC Press, Boca Raton, FL, USA, 2017.
[38] M. Zielinska, M. Markowski, D. Zielinska, The effect of freezing on the hot air and microwave vacuum drying kinetics and texture of whole cranberries, Drying Technol. 37 (13) (2019) 1714–1730.
[39] M. Zielinska, P. Sadowski, W. Błaszczak, Freezing/thawing and microwave-assisted drying of blueberries (*Vaccinium corymbosum L.*). *LWT-Food*, Science and Technology 62 (1) (2015) 555–563.
[40] M. Zielinska, D. Zielinska, M. Markowski, The effect of microwave-vacuum pretreatment on the drying kinetics, color and the content of bioactive compounds in osmo-microwave-vacuum dried cranberries (*Vaccinium macrocarpon*), Food Bioprocess Technol. 11 (3) (2018) 585–602.

Further reading

[3] Y. Ando, S. Hagiwara, H. Nabetani, I. Sotome, T. Okunishi, H. Okadome, T. Orikasa, A. Tagawa, Improvements of drying rate and structural quality of microwave-vacuum dried carrot by freeze-thaw pretreatment, LWT-Food Sci. Technol. 100 (2019) 294–299.
[14] V. Kumar, M.K. Devi, B.K. Panda, S.L. Shrivastava, Shrinkage and rehydration characteristics of vacuum assisted microwave dried green bell pepper, J. Food Process Eng. 42 (4) (2019) e13030.
[26] F. Vallespir, Ó. Rodríguez, V.S. Eim, C. Rosselló, S. Simal, Freezing pretreatments on the intensification of the drying process of vegetables with different structures, J. Food Eng. 239 (2018) 83–91.
[27] F. Vallespir, J.A. Cárcel, F. Marra, V.S. Eim, S. Simal, Improvement of mass transfer by freezing pretreatment and ultrasound application on the convective drying of beetroot (Beta vulgaris L.), Food Bioprocess Technol. 11 (1) (2018) 72–83.